

# Structural Characterization of Interfacial *n*-Octanol and 3-Octanol Using Molecular Dynamic Simulations<sup>†</sup>

Raeanne L. Napoleon and Preston B. Moore\*

Department of Chemistry & Biochemistry, University of the Sciences in Philadelphia, Philadelphia, Pennsylvania 19104

Received: August 31, 2005; In Final Form: November 21, 2005

Structurally isomeric octanol interfacial systems, water/vapor, 3-octanol/vapor, *n*-octanol/vapor, 3-octanol/water, and *n*-octanol/water are investigated at 298 K using molecular dynamics simulation techniques. The present study is intended to investigate strongly associated liquid/liquid interfaces and probe the atomistic structure of these interfaces. The octanol and water molecules were initially placed randomly into a box and were equilibrated using constant pressure techniques to minimize bias within the initial conditions as well as to fully sample the structural conformations of the interface. An interface formed via phase separation during equilibration and resulted in a slab geometry with a molecularly sharp interface. However, some water molecules remained within the octanol phase with a mole fraction of 0.12 after equilibration. The resulting “wet” octanol interfaces were analyzed using density profiles and orientational order parameters. Our results support the hypothesis of an ordered interface only 1 or 2 molecular layers deep before bulk properties are reached for both the 3-octanol and water systems. However, in contrast to most other interfacial systems studied by molecular dynamics simulations, the *n*-octanol interface extends for several molecular layers. The octanol hydroxyl groups form a hydrogen-bonding network with water which orders the surface molecules toward a preferred direction and produces a hydrophilic/hydrophobic layering. The ordered *n*-octanol produces an oscillating low–high density of oxygen atoms out of phase with a high–low density of carbon atoms, consistent with an oscillating dielectric. In contrast, the isomeric 3-octanol has only a single carbon-rich layer directly proximal to the interface, which is a result of the different molecular topology. Both 3-octanol and *n*-octanol roughen the water interface with respect to the water/vapor interface. The “wet” octanol phases, in the octanol/water systems reach bulk properties in a shorter distance than the “dry” octanol/vapor interfaces.

## 1. Introduction

Surface and interface properties are of great importance as many chemical, physical, and biological processes occur at the interfaces. Details of interfacial systems at the molecular level are especially crucial to the understanding and development of applications since a plethora of processes occur at the liquid/liquid interface. For example, processes such as biological signaling, transportation of ions or organic molecules across membranes, chromatographic separation, and surface catalytic reactions are all critically dependent on properties of the interface. The structural and dynamical properties of the interfaces have major impacts on the movement of molecules across or along an interface. Further, both structures and chemical properties of an interface can be altered by surfactant chemistry. However, the resulting perturbation to the relatively “simple” neat interface and its properties cannot be predicted easily. While interfaces are ubiquitous in chemistry and biology, the atomic level contributions to the interfacial properties (chemical and physical) are not yet fully understood. Specifically, standard experimental probes are not applicable to the liquid/liquid interface systems, and atomistic resolution of interfaces are difficult to quantify using conventional experimental methods available today.

The atomistic details of a liquid/liquid interface can be probed using molecular dynamics (MD) simulations, through which one

can gain valuable insight into the atomic structure and dynamics of interface systems. Previous MD simulations have focused heavily on the structural and physical properties of interfaces characterized by a liquid/vapor or two weakly associated immiscible liquids.<sup>1–7</sup> Simulations of strongly associating liquid/liquid interfaces such as octanol/water presented in this study are extremely scarce. There is a paucity of information on the structure of strongly associated liquid/liquid interfaces,<sup>8</sup> while the liquid/vapor<sup>6,9,10</sup> and weakly associated interfaces have been investigated to a much greater extent.<sup>2–4,6,9–13</sup>

Computer simulations have been used to study water interfaces in atomic detail for over 20 years. One such example is the pioneering work of Lee et al. which characterized the water structure at a solid hydrophobic surface and showed that ordering in water at a solid surface persists for only a few angstroms.<sup>14,15</sup> Gordillo and Martí studied the static and dynamic properties of several layers of water molecules on top of a graphite surface (a more realistic model of a hydrophobic surface)<sup>16</sup> and found results consistent with the earlier work of Lee et al., in which only one ordered water layer is proximal to the weakly associated hydrophobic interfaces.

Interfaces of water with other liquids have also been studied extensively. Chang et al. have reported in their study that weakly associated liquid/liquid interfaces, such as CCl<sub>4</sub>/H<sub>2</sub>O, show an ordering of the molecules at the interfaces.<sup>2</sup> Chipot et al. utilized a hexane/water interface to gain insight into how some common anesthetics will transfer across the interface.<sup>3</sup> Schweighofer et al. investigated sodium dodecyl sulfate (SDS) at the water/vapor

<sup>†</sup> Part of the special issue “Michael L. Klein Festschrift”.

\* To whom correspondence should be addressed. E-mail: p.moore@usip.edu.

interface as well as the water/carbon tetrachloride interface.<sup>10</sup> These results are consistent with the experimental observation of surface active molecules and a roughening of the surface. da Rocha et al. have studied the carbon dioxide/water interface<sup>4</sup> and found molecularly sharp interfaces in both the water and carbon dioxide phases. Interfaces of liquids other than water have also been reported. One such study is by Bordner et al. in which they calculated the solvation free energies of *n*-octanol and *n*-hexadecane from vapor to aqueous phase and used their results to describe solvent–solute interactions.<sup>12</sup>

Although computational studies of strongly associated liquids are limited, a recent MD simulation of *n*-octanol has been presented by Benjamin.<sup>17</sup> In this study, the structure of the *n*-octanol/water interface was investigated and ordered octanol molecules were found at the interface. A similar study employing Monte Carlo (MC) techniques has indicated that the formation of hydrogen bonds between interfacial water and octanol plays an important role in determining the properties of the *n*-octanol/water interface.<sup>7</sup>

Experimentally, it is difficult to investigate liquid interfaces in high detail due to the dominating bulk signals. However, there are techniques, such as second harmonic generation (SHG), sum frequency generation (SFG), small-angle X-ray scattering, time-resolved total internal reflection fluorometry, NMR, and neutron scattering, that can be used to probe the liquid/liquid interface.<sup>18–27</sup> The neat liquid *n*-octanol has been studied by infrared and near-infrared spectroscopy. To date, no information about the *n*-octanol/vapor or *n*-octanol/water interfaces has been reported.<sup>28</sup> Miranda et al. used SFG vibrational spectroscopy to study water/vapor and alcohol/vapor interfaces,<sup>29</sup> which provides evidence for structured water and alcohol at the interface. X-ray scattering measurements have indicated that an alcohol (tri-*n*-octanol) monolayer has a well-defined order at the water/hexane/vapor interface.<sup>13</sup> This ordering has been deduced from the distinct 10–15% increase in electron density at the alcohol interface region ( $-\text{CH}_2\text{OH}$ ) when compared to that of the water/vapor interface. The increase in electron density is attributed to water penetrating into the headgroup region of the monolayer. Steel and Walker<sup>30–32</sup> have used a surface active chromophore as a “molecular ruler” to probe a nominal interface dividing surface. They observed how changes in the solute structure at an interface can significantly affect the solute’s solvation environment.<sup>33</sup> They have hypothesized that there is a hydrocarbon-rich region at the water/octanol interface, in which the octanols are ordered.

While these experiments have given significant insight into the structure of the interface, they are difficult to perform and interpret. The experimentally observed anomalous dielectric responses at the *n*-octanol/water interface reported by Steel et al.<sup>30–33</sup> inspired us to elucidate, at atomic resolution, the interfacial spacial orientation of the water, *n*-octanol, and 3-octanol molecules using current MD methods. We present the results of this investigation in this paper. The overall goal of the present study is to gain a better understanding of the fundamental interactions at interfaces and how these interactions lead to the observed structure and dynamics which in turn control the chemical and physical properties of interfaces. The predictions from the present study should be testable with experimental techniques such as SHG, SFG, small-angle X-ray scattering, or the use of chromatic surfactants.

## 2. Methodology

We have carried out a series of computer simulations of *n*-octanol and 3-octanol employing standard MD methods.<sup>34</sup> In

**TABLE 1: LJ Potential Parameters for Octanol and Water**

atom	amber type	charge (e)	$\epsilon$ (K)	$\sigma$ (Å)
O–water	OW	−0.8476	76.4666	3.15075
H–water	HW	0.4238	0	0
O–octanol	OH	−0.798	105.846	3.06647
H–hydroxyl	HO	0.431	0	0
C–methyl	CT	0	55.0359	3.39967
C–(bonded to O)	CT	0.297	55.0359	3.39967
H–methyl	H1	0	7.8982	2.47135

each system, we model the water with a SPCF model<sup>39,43</sup> and the octanol molecules are modeled with all-atom potentials obtained from Amber95.<sup>35</sup> All molecules are fully flexible and allow for stretching, bending, and torsional motions. We report the Lennard-Jones and charge parameters in Table 1 for homogeneous atomic interactions and the usual combination rules are used for heterogeneous interactions. All systems presented here are listed in Table 2 along with the simulated and experimental bulk densities. The initial system was set up by placing all molecules (for each system) randomly in an elongated box of  $45 \times 45 \times 135$  Å. In the case of liquid/vapor interface studies, each system consisted of a total of 256 alcohol molecules. A simulation of a liquid/vapor interface of water with 2048 molecules was also carried out for comparison. In the case of alcohol/water interface studies, 2048 water molecules were added to the simulation box in addition to the 256 alcohol molecules. The number of alcohol molecules and number of water molecules were chosen to ensure sufficient bulk between the formed interfaces.

For each system, several initial configurations were equilibrated within the NPT ensemble (constant number of particles, constant pressure of 1 bar, and constant temperature of 298 K), with a time step of 1 fs using the CM3D MD simulation code developed by Moore.<sup>36</sup> The NPT ensemble is used to relieve any strains within the system resulting from close proximity of molecules and/or from spacial voids within the system as a result of the initial random placement of the molecules. Periodic boundary conditions were applied in three dimensions to minimize finite size effects. The size of the simulation box is initially  $45 \times 45 \times 135$  Å with the longest side coinciding with the *z*-axis. The asymmetric box biased the spontaneous formation of an interface perpendicular to the *z*-axis. Ewald sum techniques were employed to account for the long-range electrostatic interactions.<sup>34</sup> The final interface systems are technically an infinite series of slabs alternating phases along the *z*-direction. Each system was simulated from its initial configurations until an equilibrium was reached, which was characterized by the fluctuation of volume and each energy component around their equilibrium values.

Once each system reached equilibrium, a minimum of a 10 ns production run was carried out for each system within the NVT ensemble. The trajectories from these production runs were used for analysis. The interface thickness was characterized by fitting the atomic density as a function of distance (*z*) perpendicular to the interface using

$$\rho(z) = \frac{(\rho_a + \rho_b)}{2} + \frac{(\rho_a - \rho_b)}{2} \tanh\left(\frac{\alpha(z - z_0)}{d}\right) \quad (2.1)$$

where  $\rho_a$  and  $\rho_b$  are the densities of the two pure phases,<sup>40</sup> and the constant  $\alpha = 2 \tanh^{-1}(0.8) = 2.19722$  was chosen so that the interface width *d* is the distance between 10% and 90% of the difference in densities ( $\rho_a$  and  $\rho_b$ ) of the two pure phases. We define the liquid phase as a region with a density more than 90% of the experimental liquid density, the vapor phase

**TABLE 2: Systems Simulated and Fitted Interfacial Widths**

system	bulk density g/cm <sup>3</sup>	expt density g/cm <sup>3</sup> <sup>41</sup>	width $d$ in eq 1 (Å)			
			carbon	oxygen	diff@50%	water
water/vapor	0.97 ± 0.02	.997				4.3
3-octanol/vapor	0.84 ± 0.02	0.8258	5.6	2.1	1.6	
<i>n</i> -octanol/vapor	0.83 ± 0.01	0.8262	5.4	2.4	3.4	
3-octanol/water	0.85/0.99		6.2	2.1	−2.4	7.8
<i>n</i> -octanol/water	0.85/0.99		4.6	2.5	−3.4	5.5

as a region with a density less than 10% of the liquid density, and the interface region as a region between 10–90% liquid density.

All simulations were carried out at the University of the Sciences in Philadelphia on local linux workstations, a 32 processor Beowulf Cluster with AMD 1.666 GHz athlon processors, or a 128 processor cluster composed of dual core 2.2 Ghz AMD opteron processors using CM3D.<sup>36</sup> The estimated processing time for each system was approximately 130 days or an equivalent of 3 years of single processor for all simulations.

### 3. Results and Discussion

The systems reported in this study are listed in Table 2 along with the average bulk densities (obtained by averaging the middle 40 Å of the slab), the experimental bulk density, and the widths of the interface obtained by fits to eq 1 for each pure phase. The densities of the pure phases are close to the bulk experimental values and reflect that the potentials are reliable for these small molecular systems. The widths of the interface are reported for each atomic component of the interface. Carbon (C) represents the carbon density of the octanol, oxygen (O) represents the oxygen density of octanol, and water represents the O density of the water molecules. The “diff@50%” column in Table 2 is the difference between the C and O interface at  $1/2$  of their respective bulk values. A negative sign indicates that the O density reaches 50% before the C density reaches 50% of their respective bulk values, which indicates that a layer of oxygen atoms is at the interface. These are the first reported MD simulations of octanol interfaces, except *n*-octanol/water, of which we are aware.

**3.1. Equilibration.** Initially, all molecules (water, and/or *n*-octanol, and/or 3-octanol) are randomly placed in an elongated simulation box. All simulations proceeded similarly with an initial small clustering of similar species (water or octanol), forming small spherical domains. These small spherical domains merged to form larger and larger domains of individual molecular species. Once a domain reaches approximately 90% of the shortest box dimension (chosen to be in the  $x$ – $y$  plane), spontaneous thermal fluctuations within the spherical droplet come into contact with its own periodic image. These interac-

tions with its own periodic image facilitate a change in morphology from a spherical domain into a slab geometry. The slab geometry remains stable for the remainder of the simulations, which is expected because this morphology minimizes the surface area. The formed interface is planar, with only small deviations from planarity. After the interface has been stable for minimum of 1 ns, data is collected for analysis. We define a stable interface when the volume, each energy component (electrostatic, VDW, bonds, bends, torsions, etc.), pressure, and thickness of the slab all fluctuate around some equilibrium value.

The interface achieved by the random placement procedure is indistinguishable from the traditional procedure of forming an interface by starting with pure bulk phases in a cubic geometry and then elongating one dimension. We have simulated *n*-octanol/water and *n*-octanol/vapor systems using the traditional methods of obtaining an interface and found no significant difference in the equilibrated interface. Furthermore, we have simulated the *n*-octanol/water system at 350 K for 1 ns and then cooled the system down to 298 K. Again, we found no significant difference compared to the interface formed using the random placement method. While the interface formed in all procedures is indistinguishable, the octanol/water simulations do have a small amount of residual water in the interior of the bulk octanol phase. These water molecules were trapped in the octanol phase due to the initial random placement procedure and remained within the octanol. Conversely, while some octanol molecules were also initially trapped within the water phase during the random placement procedure, these molecules eventually diffused and joined the octanol phase. The mole fraction  $\chi$  of the water within the octanol phase is 0.12, which is close to previous simulations<sup>37</sup> but lower than the experimental value of 0.20 to 0.29.<sup>38</sup> We did see a few water molecules transferring from one phase into the other, which gives us confidence that we have reached equilibrium. Thus, our octanol simulations of the octanol/water interface result in a “wet” octanol phase instead of a “dry” one, which mimics the usual experimental octanol/water interfaces.

A snapshot of the *n*-octanol/water simulation after equilibration is shown in Figure 1. This figure shows a major conclusion of the present work, which is that the *n*-octanol interface, unlike the water and 3-octanol interfaces, has layering well beyond

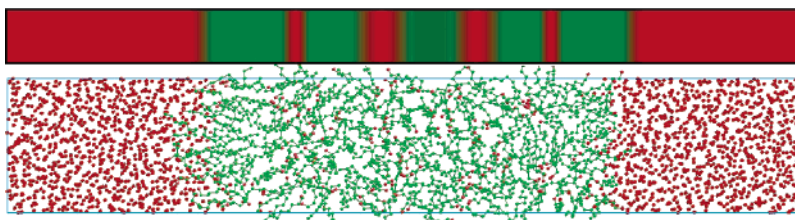


**Figure 1.** Snapshot of a representative configuration from the *n*-octanol/water system. Water and *n*-octanol are not miscible, in accordance with experimental evidence. The *n*-octanols align themselves perpendicularly to the plane of the interface so as to create a hydrogen-bonding network spanning the interface and interacting with the water hydrogen-bonding network. Doing so also protects the hydrophobic portion of the molecule from the water molecules. Unlike water/vapor, 3-octanol/vapor, and 3-octanol/water interfaces, the *n*-octanol/water interface has oscillation layers of high and low oxygen density regions as depicted in the cartoon above the snapshot. Green represents a hydrocarbon-rich region, whereas red represents an oxygen-rich region.



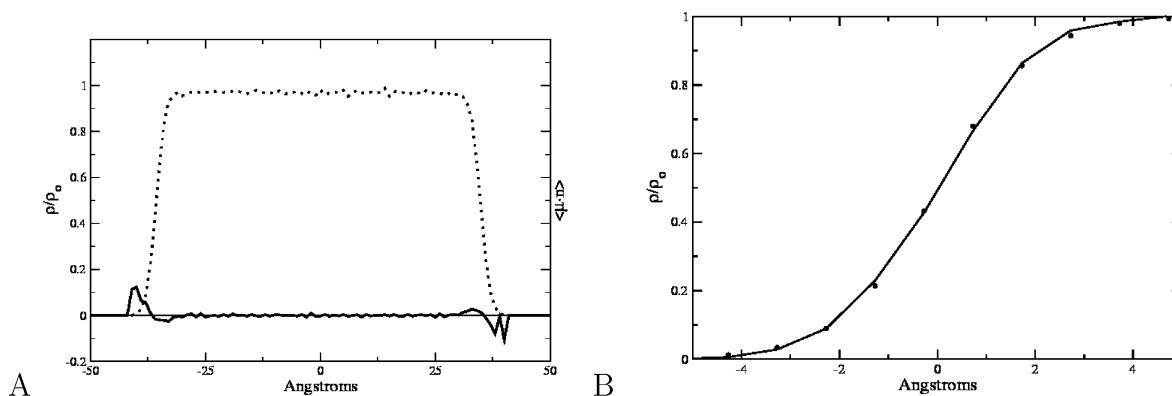


**Figure 2. Water/vapor:** (A) density profile of water across the slab (dotted line,) and the orientational parameter (solid line). The density has been normalized by average bulk density (0.97 g/cc). The solid line is the orientational order parameter of a unit vector along the dipole moment of the water molecules projected onto a unit vector perpendicular to the surface (i.e.,  $\{0,0,1\}$ ). (B) Close up of the density profile of the water/vapor interface (solid line); the points are from a fit to eq 1.

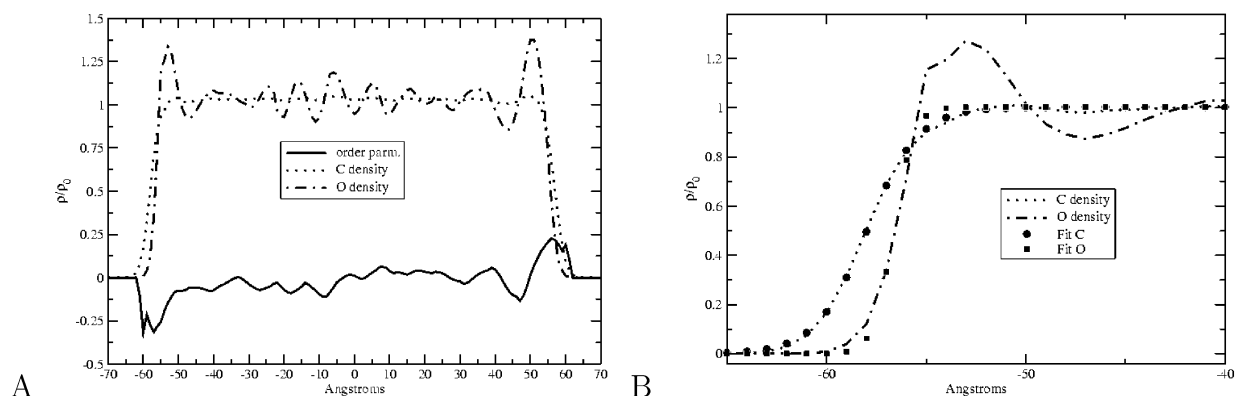


**Figure 3. 3-Octanol/vapor:** (A) 3-octanol/vapor interface density profile and orientational parameter. The densities have been normalized by their bulk values. The orientational parameter is defined as a unit vector from the oxygen atom to the farthest carbon atom dotted into a unit vector perpendicular to the interface (i.e.,  $\{0,0,1\}$ ). The solid line is the orientational vector, the dotted line is the carbon density, and the dot-dash line is the oxygen density. (B) The interface and fit to eq 1 for each component.

the interface. While molecularly sharp interfaces are observed in all simulations, that is, one phase stops and the other phase starts within a single molecular length of about 6 Å, the interface causes ordering of the *n*-octanol molecules which can persist for 75 Å into the *n*-octanol phase.

**3.2. Water/Vapor.** The water/vapor interface has been simulated and characterized in numerous MD studies.<sup>42–44</sup> Here, we reproduce what others have already reported to introduce our analysis, order parameters, and demonstrate the robustness of the current simulations. Unlike many previous simulations, which begin with a bulk phase and then elongate one dimension of the box, our initial system setup began with a random placement of water within an elongated box (see section 3.1). The equilibrium slab geometry obtained is indistinguishable from the one started from a cubic bulk water box and elongating along one dimension.

One essential water/vapor interface result is that the interface is molecularly sharp, that is, the transition from the bulk density to the vapor occurs within 1 or 2 molecular lengths. In Figure 2, we plot the density as a function of distance ( $z$ ) perpendicular to the interface. Our fit to eq 1 is excellent (Figure 2B) and gives a width of 4.3 Å for the density to go from 10% to 90% of its bulk value. The bulk density calculated from our simulation is  $0.97 \pm 0.02$  g/cm<sup>3</sup>, which is in good agreement with the experimental value of 0.998 g/cm<sup>3</sup> for water at 298 K.<sup>41</sup>

Along with the density profile in Figure 2, we report an order parameter for the water molecules as a function of distance perpendicular to the interfaces, which we define as a unit vector

along the dipole moment of the water molecule projected onto a unit vector perpendicular to the interface (i.e.,  $\{0,0,1\}$ ). The water at the interface orients to maximize the hydrogen-bonding (H-bonding) network, as evidenced by the slight deviation from zero at  $-35$  and  $35$  Å, located at the high-density side of the interface. The orientation proximal to the bulk is such that a large subset of molecules are oriented to maximize the H-bonding, as has been shown before,<sup>43</sup> which gives rise to the preferred orientation at the high-density side of the interface (Figure 2). Only about 25% of the water molecules have “dangling” H-bonds (hydrogens that are not involved in hydrogen bonding) as has been seen in previously reported simulations and experiments.<sup>29,43,45</sup> These dangling H-bonds orient themselves perpendicular to the interface. An interesting feature in Figure 2 is the two peaks at the low-density side of the interfaces ( $-39$ ,  $-37$  and  $37$ ,  $39$  Å). These peaks are from a few evaporating water molecules. The water molecules orient to H-bond with the interface antiparallel to the water proximal to the interface and parallel to the “dangling” H-bonding water molecules. The species on the low-density side of the interface are transient and either quickly evaporate into the gas phase or are reabsorbed back into the bulk.

**3.3. 3-Octanol/Vapor.** We characterized the 3-octanol/vapor interface in a similar manner as the water/vapor interface. The density profile of carbon (C) and oxygen (O) across the 3-octanol/vapor interface is reported in Figure 3. The C density profile rises sharply from zero to bulk value. The C density does have a higher than bulk value ( $-52$  and  $52$ ) region and a lower than bulk value ( $-45$  and  $45$ ) region at the interface. After

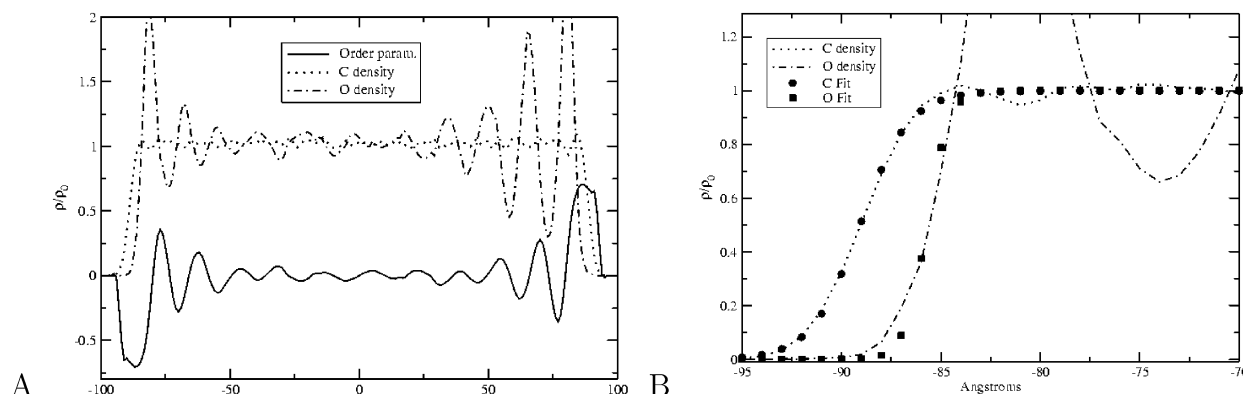


**Figure 4. *n*-Octanol/vapor:** (A) *n*-octanol/vapor interface density profile and orientational parameter. The densities have been normalized by their bulk values. The orientational parameter is defined as a unit vector from the oxygen atom to the farthest carbon atom projected onto a unit vector perpendicular to the interface (i.e., {0,0,1}). A solid line is the orientational vector, the dotted line is the carbon density, and the dot-dash line is the oxygen density. (B) The interface and fit to eq 1 for each component.

this single oscillation, the density profile is constant, suggesting bulk properties have been reached. The O density profile shows a similar rise and depletion as the C density profile. The 3-octanol has a depletion in the carbon density profile commensurate with the O depletion. This leads us to our hypothesis of an ordered molecular layer at the interface which is distinct from the bulk. The middle of the 3-octanol phase reaches a bulk density of  $0.84 \pm 0.02$  g/cm<sup>3</sup>, which compares favorably with the experimental value of 0.8258 g/cm<sup>3</sup> at 298 K.<sup>41</sup>

The width of the interface is 5.6 Å, obtained from fitting eq 1 to the C density profile. We also fit the O density profile and obtained an interfacial width of 2.1 Å, even though the interface does not smoothly transition from the liquid phase. The 2.1 Å interface width is very sharp and occurs for two reasons: (1) The oscillations in O density hinder the fitting, and a different equation might be required in order to obtain a better fit. (2) The octanol molecules H-bond to each other, giving rise to a dense layer of oxygen atoms just below the surface. There is a small hydrocarbon region (1.6 Å) covering the oxygen H-bonded layer. Bulk densities are obtained about 20 Å below the surface.

A single interface layer can also be seen in the order parameter which we define as a unit vector between the oxygen atom and the farthest carbon atom within the same octanol molecule projected onto a unit vector perpendicular to the surfaces (i.e., {0,0,1}). The small single oscillation suggests that the molecules are weakly ordered. This ordering is consistent with a hydrocarbon layering at the surface which allows for H-bonding within the middle of the first molecular layer. Below this layer, the molecules are essentially randomly ordered as expected within the bulk liquid.

**3.4. *n*-Octanol/Vapor.** We characterized the *n*-octanol/vapor (Figure 4) interface in a similar manner as the water/vapor and 3-octanol/vapor interfaces. The density profiles of C and O atoms of the *n*-octanol show that the molecules are oriented with a hydrophobic layer (carbon-rich layer) at the interface. The carbon interfacial width is 5.4 Å, which is less than a single molecular length. There is an initial layer of carbon atoms above a layer of oxygen atoms (3.4 Å at 50 bulk density), thus exposing a hydrophobic layer to the vapor phase. The hydrocarbon portion of the molecules "coating" the interface is well-known. For example, in colloids<sup>46</sup> or surfactants,<sup>17</sup> a hydrocarbon-rich layer exists at the interface.

The O density profile has significant structure. As in the 3-octanol/vapor interface, the O width of 2.4 Å is extremely sharp for a layer of high oxygen density. Just below the surface, there are more oxygen atoms that H-bond to hydroxyl groups on other molecules, resulting in an oxygen-enriched layer with

an O density twice as much as the bulk oxygen density. The O density profile then oscillates around the bulk value until 75 Å into the liquid phase. The C density profile has a similar feature to that of the O density profile. There is a sharp vapor to bulk density transition and a few oscillations (less pronounced) out of phase with the O density. While the *n*-octanol/vapor interface is molecularly sharp with only 5.4 Å to go from 10% to 90% bulk density, the transition to truly isotropic bulk density occurs over many layers. Thus, unlike the water interface, there is a residual order 75 Å from the interface. We see evidence of 4 to 5 layers of oscillation high-low density of O before flat bulk values are obtained in the oxygen density. This *n*-octanol layering was unexpected. We expected the trans-gauche defects and orientational thermal fluctuations to blur the interface over very short length scales. Our simulations support the idea that the stacking and H-bonding between molecules are enough to induce ordering and overcome any entropic barriers. The bulk density within the middle of the slab is  $0.83 \pm 0.01$  g/cm<sup>3</sup>, which compares favorably with the experimental density of 0.8262 g/cm<sup>3</sup>.<sup>41</sup>

Layering can also be seen in the order parameter. We define the order parameter, similar to the one used in the 3-octanol case, as a unit vector between the oxygen atom and the farthest carbon atom on the same molecule projected onto a unit vector perpendicular to the surface. Again, in contrast to water (section 3.2) and 3-octanol (section 3.3) reported above and consistent with the O density profile, the interface persists for many atomic layers with oscillating orientation. The orientation vector oscillates positively and negatively as the molecules orient themselves in a head-to-head type of stacking to facilitate H-bonding. These orientations correlate with the oxygen atom density (Figure 4). Such correlations are anticipated as the *n*-octanol molecules involved in H-bonding need to have the O atoms within the same layer. Similar to the water interface, we see a few molecules evaporate from the surface during the course of the simulation. In these relatively rare events, the molecules diffuse out from the interface due to thermal fluctuations. This motion causes the narrow sharp peaks at the interface (−90 and 90). However, the statistics are very poor since fewer than 5 molecules were observed evaporating off the surface. We predict that the peak position from these transient events will be blurred by capillary waves within the slab on longer runs or larger simulations.

The molecular topology of a hydrophilic end attached to a hydrophobic chain strongly aligns the molecules at the surface similar to a monolayer or self-assembled monolayer (SAM). This strong ordering causes purely hydrophilic (high oxygen

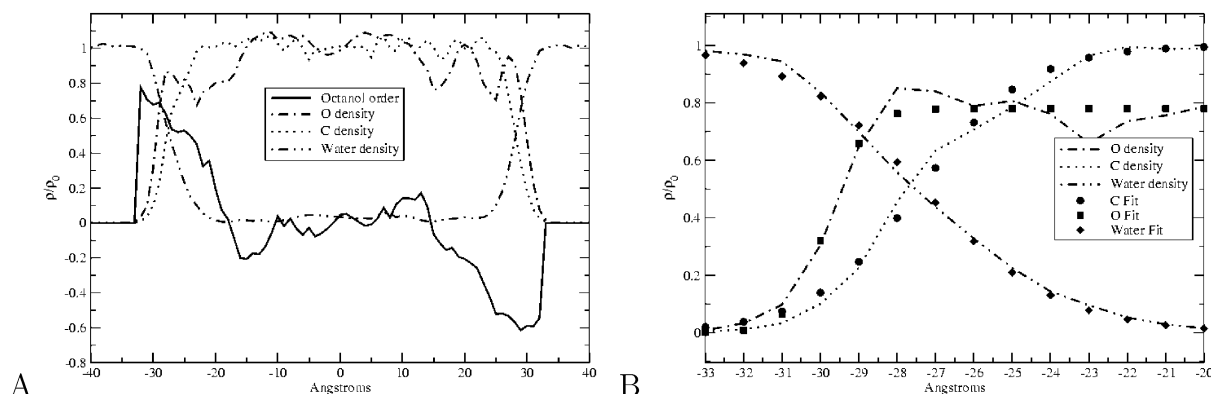


**Figure 5. 3-Octanol/water:** (A) 3-octanol/water interface density profile and orientational parameter. The densities have been normalized by their bulk values. The orientational parameter is defined as a unit vector from the oxygen atom to the furthest carbon atom dotted into a unit vector perpendicular to the interface (i.e.,  $\{0,0,1\}$ ). The solid line is the orientational vector, the dotted line is the 3-octanol carbon density, and the dot-dash line is the 3-octanol oxygen density. (B) The interface and fit to eq 1 for each component.

density) layering just below the surface as the hydroxyl group repelled from the hydrocarbon layer. The next layer will preferentially orient in an antiparallel fashion to the surface molecules resulting in a bilayer-type structure. This series of steps is repeated several times to give layering and density fluctuations much farther from the interface than either water/vapor or 3-octanol/vapor exhibit.

In bulk *n*-octanol, energetically favorable H-bonds form between molecules. These H-bonds form chains of varying length resulting in wormlike structures within the bulk. However, at the interface, the homogeneous symmetry of the bulk is broken and the *n*-octanol molecules orient perpendicular to the interface causing layering instead of the bulk wormlike structures to form. The interface oscillates at least four times before transitioning back to bulk behavior. As seen previously,<sup>7,17</sup> the *n*-octanol molecules that tend to be oriented perpendicular to the interface are those that are H-bonded. Those that are not H-bonded are randomly ordered, the degree to which they are ordered is dependent on the definition of the H-bonding that we use. However, regardless of the definition, there is a slight preference for the orientation perpendicular to the interface. This can be rationalized by the fact that in order for molecules to diffuse or flip the H-bonding will be broken. However, there will still be residual order which causes the slight orientational preference, similar to the H-bonding molecules.

While 3-octanol and *n*-octanol are isomers with identical chemical formula ( $C_8H_{18}O$ ), their topologies (bonding configurations) are different, which leads to a difference in the interfacial properties. The *n*-octanol is able to stack and closely pack its hydrocarbon tails, thus increasing the ordering due to its topology of a hydrophilic head and a hydrophobic tail. 3-Octanol has a different topology which does not allow for strong packing and ordering, with two short tails instead of one long tail. The 3-octanol topology results in an interface similar to that of water in which the density and orientational parameters deviate from the bulk for only a single molecular layer. Beyond this interfacial layer, both the orientation parameter and density reach their bulk values.

**3.5. 3-Octanol/Water.** With the structure of the 3-octanol/vapor interface characterized (section 3.3), we compare it to the 3-octanol/water interface. The density profile of C and O of 3-octanol shows that the 3-octanol molecules are oriented at the interface with an O layer instead of the C layer as in the case of the liquid/vapor interface (Figure 5). This is evident from the oxygen density rising before the carbon density. The 3-octanol molecules are oriented  $180^\circ$  with respect to the liquid/vapor interface (compare Figure 3 with Figure 5). Unlike the

3-octanol/vapor interface, there is strong ordering at the 3-octanol/water interface as the molecule H-bonds to water molecules at the interface. The strong H-bonding causes the molecules to align. However, due to its topology, close packing of the 3-octanol molecules is not possible, which results in a decrease of both the O and C densities at the interface. In addition, the interface is broadened compared to the liquid/vapor interface, as evidenced by the width of the interface of 6.2 vs 5.6 Å. After a single interfacial molecular layer, the system obtains bulk properties and no strong ordering as evidenced by the constant featureless density profiles.

The ordering of the 3-octanol molecules at the interface is also observed in the order parameter, in which only two oscillations are seen before random bulk values are observed. A value of 0.8 in the order parameter is evidence of very well-ordered octanol molecules. The order persists for over 10 Å before flipping directions indicating that there is a hydrocarbon region at the interface. This hydrocarbon region is supported by the C and O density profiles.

The water interface at the 3-octanol/water interface is roughened with respect to the water/vapor interface, as evidenced by the width of 7.3 vs 4.3 Å. The 3-octanol molecules oriented to H-bond with the water phase. However, due to the topology of the molecules, the packing at the interface leaves pockets which are filled by water molecules. Due to the simulation protocol used to set up the unbiased interface, we are simulating a “wet” 3-octanol vs a “dry” 3-octanol/water interface. The inclusion of water molecules in the 3-octanol phase does not perturb the interface in any detectable way. We obtain identical (within statistical error) density profiles and order parameters as with a “dry” 3-octanol/water interface. However, the water molecules do disturb the bulk octanol chains by H-bonding to the octanol hydroxyl groups and shortening the average octanol H-bonding chain length. This disturbance allows for bulk “wet” properties to be reached in a shorter distance than that with the 3-octanol/vapor case.

**3.6. *n*-Octanol/Water.** With the liquid/vapor interface characterized, we compare the liquid *n*-octanol/water interface. Our results are consistent with a previous MD study of *n*-octanol by Benjamin.<sup>17</sup> There are both oxygen- and carbon-rich layers (Figure 6) at the interface. The *n*-octanol/water interface is different from the *n*-octanol/vapor interface in that the oxygen-rich layer comes before the carbon-rich layer (— sign in the diff@50%). This is due to the *n*-octanol molecules orienting to H-bond with the water molecules, which is  $180^\circ$  from the *n*-octanol/vapor case. However, similar to the *n*-octanol/vapor interface, we find several ordered layers of *n*-octanol which have

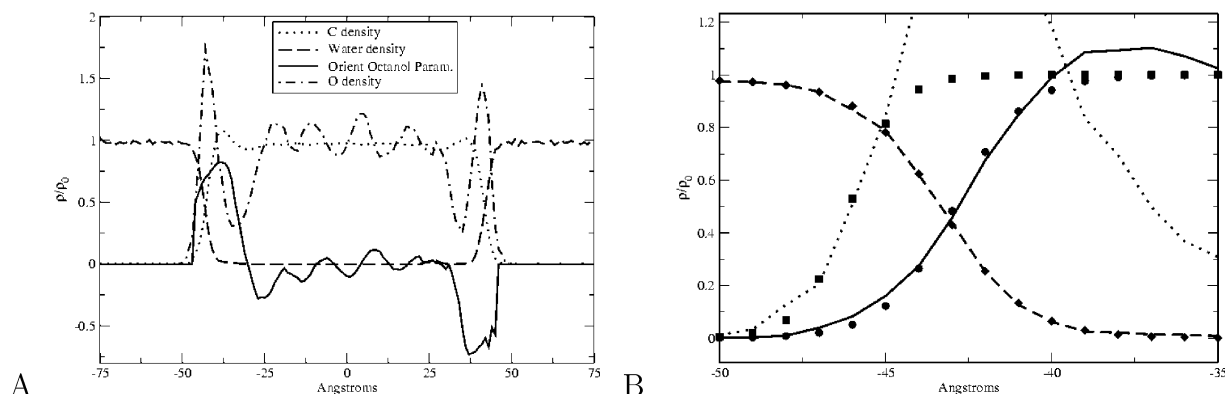


**Figure 6. *n*-Octanol/water:** (A) *n*-octanol/water interface density profile and orientational parameter. The densities have been normalized by their bulk values. The solid line is the orientational vector, the dotted line is the carbon density, the dot–dash line is the octanol oxygen density, and the dash–dash line is the water density. (B) The interface and fit to eq 1 for each component.

never been reported. Figure 1 depicts a snapshot of the *n*-octanol/water system and a cartoon of the layering within our *n*-octanol slab. Figure 6 reports the density profiles and *n*-octanol order parameter. Similarly to the *n*-octanol/vapor interface there is an enriched and a depleted region of carbon at the interface. The O density profile has a dominating peak at the interface with 50% more density than its bulk value. This is evidence of the strong ordering at the interface. There is also a region of depleted oxygen density just within the octanol side of the interface as anticipated for hydrocarbon-rich layers. This region of low-density oxygen atoms and high-density carbon atoms is the region hypothesized by Steel et al.<sup>30–32</sup> However, we predict that the oxygen density oscillates for several layers before obtaining its constant bulk value.

The *n*-octanol ordering can also be observed in the orientational parameter, which we defined in section 3.4. There is a strong ordering of the *n*-octanols at the interface and several layers into the pure *n*-octanol phase. The ordering correlates with the oxygen density in a similar manner as observed in the liquid phase of the *n*-octanol/vapor system. The *n*-octanol molecules are oriented 180° from the vapor case, as seen when comparing Figure 6 with Figure 4.

The water side of the interface is also different from the water/vapor interface. These liquids are strongly associating and H-bond within the interfacial region. This H-bonding slightly roughens the surface and removes the “dangling” H-bond that was present in the water/vapor interface. We fit the water density to eq 1 and obtain an excellent agreement with our simulation results as seen in Figure 6. We obtain a value of 5.5 Å for the width of the interface which corresponds to a slight roughening with respect to the water/vapor interface (4.3 Å).

The middle of the *n*-octanol phase reaches a bulk density of 0.85 g/cm<sup>3</sup> and that of the water phase in the middle reaches a bulk density of 0.99 g/cm<sup>3</sup>. While our bulk *n*-octanol density might seem a little high for the octanol phase, there are a few water molecules that are within the bulk phase. These few water molecules which correspond to a mole fraction ( $\chi$ ) of 0.12 are similar to previous simulations and reasonably close to the experimental value of 0.20 to 0.29 for “wet” octanol.<sup>38</sup> Further, the water molecules within the octanol phase are found to be H-bonded to octanol molecules, as seen previously.<sup>37</sup> These waters within the octanol phase disturb the ordering and layering slightly, and we see only three ordered layers of *n*-octanol compared to five layers in the pure *n*-octanol/vapor interface.

#### 4. Conclusions

We have simulated 3-octanol and *n*-octanol at the vapor and water interfaces. These are the first MD simulations of *n*-octanol/vapor, 3-octanol/vapor, “wet” 3-octanol/water, and “wet” *n*-octanol/water interfaces of which we are aware. The two isomers (*n*-octanol and 3-octanol) show different interfacial properties due to their different molecular topologies. *n*-Octanol/vapor has many layers which are the result of packing and ordering at the interface. 3-Octanol, much like water, has a molecularly sharp interface and goes from vapor to bulk in a single molecular distance of 10 Å. These results highlight the importance of molecular topology to interfacial systems. These simulations call into question the use of continuum descriptions of liquids to characterize interfacial properties. The interface is very different from the bulk and is not a simple function of either bulk phase. This major difference is in the ordering of the molecules which persist for many molecular lengths.

The water at the octanol/water interface is roughened, as seen by the width of the interfaces. Due to the H-bonding and topology of the 3-octanol, the water interface is roughened by a greater extent compared to the *n*-octanol/water interface. Molecular dynamics simulations are a powerful technique to investigate the structure of the interface. Future studies will focus on the dynamics of the interface, such as the different lateral and perpendicular diffusions. The conclusions presented here should be testable via modern techniques such as SFG spectroscopy or small-angle X-ray scattering.

**Acknowledgment.** The authors acknowledge that this research was supported in part by a gift from the H.O. West Foundation, a grant from the University of the Sciences in Philadelphia (USP), and a grant from the National Science Foundation (CHE-0420556). The authors are thankful for many useful discussions with Dr. Zhiwei Liu and Dr. Niny Rao. Finally, the authors thank Professor Micheal L. Klein for his many years of guidance, support, and friendship which have lead to research such as that presented herein.

#### References and Notes

- (1) Viecelli, J.; Benjamin, I. Adsorption at the interface between water and self-assembled monolayers: Structure and electronic spectra. *J. Phys. Chem. B* **2002**, *106*, 7898–7907.
- (2) Chang, T.-M.; Dang, L. X. Molecular dynamics simulations of CCl<sub>4</sub>–H<sub>2</sub>O liquid–liquid interface with polarizable potential models. *J. Chem. Phys.* **1996**, *104* (17), 6772–6783.



- (3) Chipot, C.; Wilson, M. A.; Pohorille, A. Interactions of anesthetics with the water-hexane interface: A molecular dynamics study. *J. Phys. Chem. B* **1997**, *101*, 782–791.
- (4) da Rocha, S. R. P.; Johnston, K. P.; Rossky, P. J. Surfactant modified CO<sub>2</sub>-water interface: A molecular view. *J. Phys. Chem. B* **2002**, *106*, 13250–13261.
- (5) Senapati, S.; Berkowitz, M. L. Computer simulations study of the interface width of the liquid/liquid interface. *Phys. Rev. Lett.* **2001**, *87*, 176101.
- (6) Benjamin, I. Solvent effects on electronic spectra at liquid interfaces. A continuum electrostatic model. *J. Phys. Chem. A* **1998**, *102*, 9500–9506.
- (7) Jedlovzky, P.; Varga, I.; Gilányi, T. Adsorption of 1-octanol at the free water surface as studied by Monte Carlo simulation. *J. Chem. Phys.* **2004**, *120* (24), 11839–11851.
- (8) López Cascales, J. J.; Berendsen, H. J. C.; García de la Torre, J. Molecular dynamics simulation of water between two charged layers of dipalmitoylphosphatidylserine. *J. Phys. Chem.* **1996**, *100*, 8621–8627.
- (9) Khare, R.; Sum, A. K.; Nath, S. K.; de Pablo, J. J. Simulation of vapor-liquid-phase equilibria of primary alcohols and alcohol-alkane mixtures. *J. Phys. Chem. B* **2004**, *108*, 10071–10076.
- (10) Schweighofer, K. J.; Essmann, U.; Berkowitz, M. Simulation of sodium dodecyl sulfate at the water-vapor and water-carbon tetrachloride interfaces at low surface coverage. *J. Phys. Chem. B* **1997**, *101* (3793–3799).
- (11) Roney, A. B.; Space, B.; Castner, E. W.; Napoleon, R. L.; Moore, P. B. A molecular dynamics study of aggregation phenomena in aqueous *n*-propanol. *J. Phys. Chem. B* **2004**, *108*, 7389–7401.
- (12) Bordner, A. J.; Cavasotto, C. N.; Abagyan, R. A. Accurate transferable model for water, *n*-octanol, and *n*-hexadecane solvation free energies. *J. Phys. Chem. B* **2002**, *106*, 11009–11015.
- (13) Tikhonov, A. M.; Schlossman, M. L. Surfactant and water ordering in triacontanol monolayers at the water-hexane interface. *J. Phys. Chem. B* **2003**, *107*, 3344–3347.
- (14) Lee, C. Y.; McCammon, J. A.; Rossky, P. J. The structure of liquid water at an extended hydrophobic surface. *J. Chem. Phys.* **1984**, *80* (9), 4448–4455.
- (15) Lee, S. H.; Rossky, P. J. A comparison of the structure and dynamics of liquid water at hydrophobic and hydrophilic surfaces – a molecular dynamics simulation study. *J. Chem. Phys.* **1994**, *100* (4), 3334–3345.
- (16) Gordillo, M. C.; Martí, J. Molecular dynamics description of a layer of water molecules on a hydrophobic surface. *J. Chem. Phys.* **2002**, *117* (7), 3425–3430.
- (17) Benjamin, I. Polarity of the water/octanol interface. *Chem. Phys. Lett.* **2004**, *393*, 453–456.
- (18) Wang, H.; Borguet, E.; Eienthal, K. B. Polarity of liquid interfaces by second harmonic generation spectroscopy. *J. Phys. Chem. A* **1997**, *101*, 713–718.
- (19) Eienthal, K. B. Photochemistry and photophysics of liquid interfaces by second harmonic spectroscopy. *J. Phys. Chem.* **1996**, *100*, 12997–13006.
- (20) Wang, H.; Borguet, E.; Eienthal, K. B. Generalized interface polarity based on second harmonic generation spectroscopy. *J. Phys. Chem. B* **1998**, *102*, 4927–4932.
- (21) Corn, R. M.; Higgins, D. A. Optical second harmonic generation as a probe of surface chemistry. *Chem. Rev.* **1994**, *94*, 107–125.
- (22) Zhuang, X.; Miranda, P. B.; Kim, D.; Shen, Y. R. Mapping molecular orientation and conformation at interfaces by surface nonlinear optics. *Phys. Rev. B* **1999**, *59* (19), 632–640.
- (23) Tichonov, A. M.; Mitrinovic, D. M.; Li, M.; Huang, Z.; Schlossman, M. L. An X-ray reflective study of the water-docosane interface. *J. Phys. Chem. B* **2000**, *104*, 6336–6339.
- (24) Zhang, Z.; Mitrinovic, D. M.; Williams, S. M.; Huang, Z.; Schlossman, M. L. X-ray scattering from monolayers of F(CF<sub>2</sub>)<sub>10</sub>(CH<sub>2</sub>)<sub>2</sub>-OH at the water-(hexane solution) and water-vapor interfaces. *J. Chem. Phys.* **1999**, *110*, 7421–7432.
- (25) Ishizaka, S.; Kim, H.-B.; Kitamura, N. Time-resolved total internal reflection fluorometry study on polarity at a liquid/liquid interface. *Anal. Chem.* **2001**, *73*, 2421–2428.
- (26) El Seoud, O. A. Use of NMR to probe the structure of water at interfaces of organized assemblies. *J. Mol. Liq.* **1997**, *72*, 85–103.
- (27) Lee, L. T.; Langevin, D.; Mann, E. K.; Farnoux, B. Neutron reflectivity at liquid interfaces. *Physica B* **1994**, *198*, 83–88.
- (28) Paolantoni, M.; Sassi, P.; Morresi, A.; Cataliotti, R. S. Infrared study of 1-octanol liquid structure. *Chem. Phys.* **2005**, *310*, 169–178.
- (29) Miranda, P. B.; Shen, Y. R. Liquid interfaces: A study by sum-frequency vibration spectroscopy. *J. Phys. Chem. B* **1999**, *103*, 3292–3307.
- (30) Steel, W. H.; Walker, R. A. Measuring dipolar width across liquid-liquid interfaces with ‘molecular rulers’. *Nature* **2003**, *424*, 296.
- (31) Steel, W. H.; Beildeck, C. L.; Walker, R. A. Solvent polarity across strongly associating interfaces. *J. Phys. Chem. B* **2004**, *108*, 16107–16116.
- (32) Steel, W. H.; Damkaci, F.; Nolan, R.; Walker, R. A. Molecular rulers: New families of molecules for measuring interfacial widths. *J. Am. Chem. Soc.* **2002**, *124*, 4824–4831.
- (33) Steel, W. H.; Walker, R. A. Solvent polarity at an aqueous/alkane interface: The effect of solute identity. *J. Am. Chem. Soc.* **2003**, *125*, 1132–1133.
- (34) Allen, M. P.; Tildesley, D. J. *Computer Simulations of Liquids*; Oxford: Oxford, U.K., 1989.
- (35) Cornell, W. D.; Cieplak, P.; Bayly, C. I.; Gould, I. R.; Merz, K. M.; Ferguson, D. M.; Spellmeyer, D. C.; Fox, T.; Caldwell, J. W.; Kollman, P. A second generation force field for the simulations of proteins, nucleic acids, and organic molecules. *J. Am. Chem. Soc.* **1995**, *117*, 5179–5197.
- (36) Moore, P. B. *CM3D molecular dynamics code*; <http://hydrogen.usip.edu/cm3d>, 2000.
- (37) Chen, B.; Siepmann, J. I. Partitioning of alkane and alcohol solvents between water, (dry or wet) 1-octanol. *J. Am. Chem. Soc.* **2000**, *122*, 6464–6467.
- (38) Sangster, J. *Octanol-Water partitioning coefficients: Fundamentals and Physical Chemistry*; John Wiley & Sons: Chichester, U.K., 1997.
- (39) Moore, P. B.; Ahlborn, H.; Space, B. A combined time correlation function and instantaneous normal mode investigation of liquid-state vibrational spectroscopy. In *Liquid Dynamics Experiment, Simulation and Theory*; Fayer, M. D., Fourkas, J. T., Eds.; ACS Symposium Series: New York, 2002.
- (40) Duque, D.; Pámies, J. C.; Vega, L. F. Interfacial properties of Lennard-Jones chains by direct simulation and density gradient theory. *J. Chem. Phys.* **2004**, *121*, 11395–11401.
- (41) Lide, D. R., Ed. *Handbook of Chemistry and Physics*, 75th ed.; CRC Press: Boca Raton, FL, 1994.
- (42) Jungwirth, P.; Tobias, D. J. Ions at the air/water interface. *J. Phys. Chem. B* **2002**, *106* (25), 6361–6373.
- (43) Perry, A.; Ahlborn, H.; Space, B.; Moore, P. B. A combined time correlation function and instantaneous normal mode study of the sum frequency generation spectroscopy of the water/vapor interface. *J. Chem. Phys.* **2003**, *118* (18), 8411–8419.
- (44) Reimers, J. R.; Watts, R. O. The structure and vibrational-spectra of small clusters of water-molecules. *Chem. Phys.* **1984**, *85* (1), 83–112.
- (45) Kuo, I.-F. W.; Mundy, C. J. An ab initio molecular dynamics study of the aqueous liquid-vapor interface. *Science* **2004**, *303*, 658–660.
- (46) Dubertret, B.; Skourides, P.; Norris, D. J.; Noireaux, V.; Brivannlou, A. H.; Libchaber, A. In vivo imaging of quantum dots encapsulated in phospholipids micelles. *Science* **2002**, *298* (5599), 1759–1762.